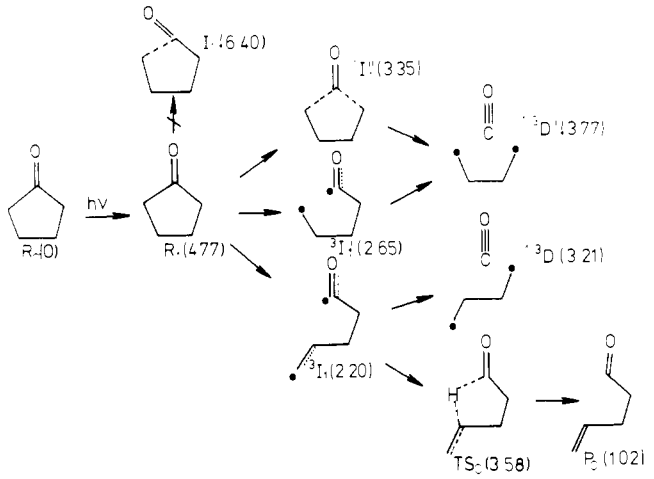

Figure 12. Schematic representation of cyclopentanone photoreaction mechanism.

quasi-degeneracy of HOMO and LUMO as can be seen from Figure 11. We have taken here two representative reactions and calculated their MO correlation diagrams with a multiconfigurational variation of moments (MCM) method.[26] These correlation diagrams show that thermal isomerization and fragmentation are Woodward-Hoffmann forbidden.[27]

A schematic survey of our results is presented in Figure 12. The figure shows the sequence of steps from reactant to products. The two diradicals ^{1,3}D and ^{1,3}D′ finish with formation of cyclobutane or two ethylene and CO.

4. Conclusion

In this investigation we have clarified the mechanism of photochemical reaction of cyclopentanone to three different products. We have presented the various pathways for photoisomerization to 4-pentenal and for photofragmentation to cyclobutane or two ethylene and CO. In all reactions excitation is followed by intersystem crossing and internal conversion. Cyclopentanone is usually the main product due to fluorescence and relaxation to the lowest triplet intermediate $^3I_1$. The products P_0, ^{1,3}D, and ^{1,3}D′ are obtained if reaction can take place before relaxation to $^3I_1$. At high excitation energies the main products are cyclobutane or two ethylene and CO in the ground state. With decreasing excitation energies, 4-pentenal is also formed.

Acknowledgment. This work was partly supported by Deutsche Forschungsgemeinschaft. One of us (P.C.M.) thanks Alexander von Humboldt-Stiftung for a fellowship. The calculations were performed with a CYBER 76 at Universität Hannover.

Registry No. Cyclopentanone, 120-92-3.

(26) Müller-Remmers, P. L.; Jug, K. *J. Am. Chem. Soc.*, submitted for publication.

(27) Woodward, R. B.; Hoffmann, R. "The Conservation of Orbital Symmetry", Verlag Chemie: Weinheim, 1971.

Properties and Reactions of Organometallic Fragments in the Gas Phase. Ion Beam Studies of FeH^+

L. F. Halle, F. S. Klein,[1] and J. L. Beauchamp*

Contribution No. 6813 from the Arthur Amos Noyes Laboratory of Chemical Physics, California Institute of Technology, Pasadena, California 91125. *Received July 28, 1983*

Abstract: Analysis of the thresholds for the reactions of Fe^+ with H_2 and D_2 studied with an ion beam apparatus yield the bond dissociation energy $D°(Fe^+–H) = 59 \pm 5$ kcal/mol. From this bond strength the proton affinity of an iron atom, PA(Fe) $= 190 \pm 5$ kcal/mol, is calculated. Ion beam studies of the deprotonation of FeH^+ by bases of various proton affinities are consistent with this value. Hydride transfer reactions of these bases with FeH^+ yield a lower limit for the hydride affinity of FeH^+, $D°(HFe^+–H^-) > 232$ kcal/mol. These energetics indicate that oxidative addition of H_2 to an iron atom is exothermic by at least 22 kcal/mol. The nearly thermoneutral formation of FeD^+ in the reaction of FeH^+ with D_2 occurs only with a small cross section at higher energies and exhibits a threshold of 20 ± 7 kcal/mol. If oxidative addition of D_2 to iron precedes reductive elimination of HD, then this activation energy implies a significant barrier for formation of an Fe(IV) intermediate. Alternatively, if the exchange process involves a four-center transition state, the observation of a significant activation energy is consistent with recent theoretical predictions that such processes are unfavorable if the metal–hydrogen bond has predominantly metal s or p character. Correlations of experimental bond energies with promotion energies provide evidence that the $Fe^+–H$ bond is primarily metal s in character. Formation of FeD^+ is observed with a moderate cross section at low energies in the reaction of FeH^+ with ethene-d_4. This results from reversible olefin insertion into the metal hydrogen bond, a process which does not involve higher oxidation states of iron. Reactions of FeH^+ with several alcohols, aldehydes, ethers, and alkanes are also presented. Facile oxidative addition reactions to C–C and C–H bonds of alkanes do not occur at low energies, presumably owing to the requisite formation of an Fe(IV) intermediate. The reactions of FeH^+ with the oxygenated compounds are generally of the type expected for strong Lewis acids.

Introduction

Activation of molecular hydrogen by a metal center is an important step in catalytic processes both in solution and on surfaces.[2] Because of this, the properties and reactivity of the intermediate metal hydrides are of great interest. Additional interest stems from the observation of diatomic metal hydrides, such as FeH, in spectra of stellar atmospheres.[3,4] These species have been

(1) On leave from the Weizmann Institute, Rehovot, Israel.
(2) Vaska, L.; Werneke, M. F. *Trans. N. Y. Acad. Sci., Ser. 2* **1971**, *33*, 70, and references therein.
(3) Smith, R. E. *Proc. R. Soc. London, Ser. A* **1973**, *332*, 113.
(4) Wing, R. F.; Ford, W. K. *Publ. Astron. Soc. Pac.* **1969**, *81*, 527.

0002-7863/84/1506-2543$01.50/0

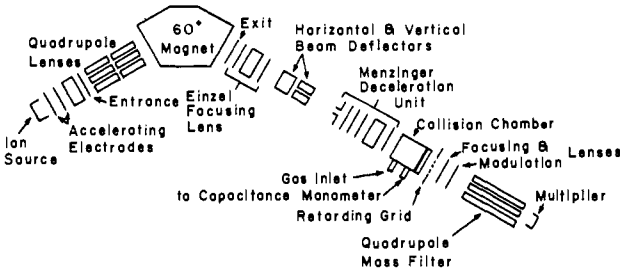

Figure 1. Schematic drawing of the ion beam apparatus.

observed in matrix isolation experiments,[5] and several theoretical papers have explored their electronic structures.[6] Metal hydrides have also been studied by using ion cyclotron resonance spectroscopy[7a] and electron photodetachment techniques.[8] Using an ion beam apparatus, we have prepared metal ion hydrides in the gas phase by the endothermic reactions of the atomic metal ions with hydrogen.[9-11] Interpretation of the threshold for this process yields the bond energy for the metal hydride ion. From this bond energy the base strength, or proton affinity (PA), of the metal can be calculated. The present work reports the results of this analysis for Fe^+.

Further reactions of the ionic products formed in the collision chamber cannot be studied with our present apparatus. However, a beam consisting of FeH^+ can be generated in the source region from electron impact fragmentation of 1,1'-dimethylferrocene. Using this approach, the reactions of FeH^+ have been examined. Ion cyclotron resonance (ICR) studies of the deprotonation of diatomic transition metal hydride ions have been used to quantify the proton affinities of metal atoms and complexes.[7,12] Similar experiments using the ion beam apparatus are reported here for the deprotonation of FeH^+ by various bases. The limits given for PA(Fe) agree well with the value calculated from the metal ion–hydrogen homolytic bond dissociation energy determined from the analysis of the reaction of Fe^+ with H_2 and D_2.

Exothermic hydride transfer reactions have also been examined; these experiments provide limits for the hydride affinity of FeH^+, $D°(HFe^+-H^-)$, which are discussed in terms of the stability of FeH_2. The reactions of FeH^+ with several alcohols, aldehydes, ethers, and alkanes are reported. In contrast to the reactions of bare group 8 transition metal ions,[10,12] facile exothermic bond insertion processes are not observed; instead reactions characteristic of a strong Lewis acid are observed.

Experimental Section

The ion beam apparatus, described in detail elsewhere,[13] is shown schematically in Figure 1. The reactant ions are mass analyzed using a 60° sector magnet which provides unit mass resolution to greater than 100 m/z. This mass-selected beam is decelerated to the desired energy and focused into a collision chamber containing the reactant gas. Product ions exit the chamber and are focused into a quadrupole mass filter and detected using a Channeltron electron multiplier operated in a pulse counting mode. Ion signal intensities are corrected for the mass discrimination of the quadrupole mass filter.

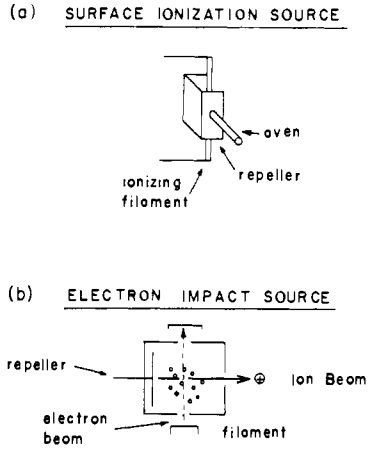

Figure 2. Schematic drawing of (a) the surface ionization source, and (b) the electron impact source.

The surface ionization source used to generate atomic iron ions[13] is sketched in Figure 2a. The oven, a stainless steel tube 1 cm long with $^1/_8$-in. i.d., is attached to a U-shaped repeller. The sides of the repeller have dimensions 10 mm × 7 mm and are spaced 5 mm apart. A rhenium ribbon (0.03 in. wide × 0.0012 in. thick) is used for the filament (~12 mm long). In these experiments, the oven is loaded with $FeCl_3$. The filament generates enough heat to vaporize the complex. The metal chloride vapor is directed at the filament where dissociation and ionization of the resulting Fe occurs. This method of ionization minimizes the production of excited metal ion states. It is estimated that at the filament temperature used, ~2500 K, 77% of the Fe^+ ions produced are in the ^6D ground state manifold and 22% are in the ^4F excited state manifold at 0.232 eV.[14]

The FeH^+ ion is formed from 1,1-dimethylferrocene by electron impact. All experiments were done at an electron energy of 70 eV unless otherwise noted. This source, sketched in Figure 2b, is of standard design in which an ion beam is extracted at a right angle from an electron beam with the aid of a small repeller field. The source is easily disassembled and cleaned. The inner dimensions of the surrounding chamber are approximately 5 mm × 6 mm × 5 mm. The rhenium ribbon described above is also used for this filament, which is 4 mm long.

Electron impact ionization of organometallic compounds has been known to create electronically excited metal ions.[15] In addition, the FeH^+ ion formed by electron impact may possess some excess vibrational energy. When proton transfer and deuterium exchange reactions were monitored as a function of electron impact energy (~30–70 eV), no change in cross section was noted. This suggests excited-state reactions of FeH^+ are not observed.

The FeH^+ ion was first reported to appear in the mass spectrum of $(CH_3C_5H_4)_2Fe$ by Mysov et al.[16] The hydride of the major isotope of iron, $^{56}FeH^+$, coincides with a minor isotope of iron, $^{57}Fe^+$(2.19%). Because of possible competing reactions from $^{57}Fe^+$, we found it more convenient at times to use $^{54}FeH^+$ as our reactant ion beam. This ion beam (mass 55) was not pure $^{54}FeH^+$, as indicated by fragmentation products at mass-to-charge ratios of 27, 29, and 39 which were observed when this ion beam was directed into the collision cell containing a nonreactive gas such as Ar. The impurity is most likely $C_4H_7^+$, an ion produced by the electron impact fragmentation of the methylcyclopentadienyl rings of $(CH_3C_5H_4)_2Fe$. A beam of $C_4H_7^+$ can be formed from electron impact of *trans*-2-butene. From a comparison of the fragmentation pattern of this $C_4H_7^+$ species upon collision with Ar to that of the 55 amu ion formed from $(CH_3C_5H_4)_2Fe$ (the patterns were similar but not identical), we estimate that 10% of the beam at 55 amu formed from the iron compound is due to $C_4H_7^+$. The interactions of the $C_4H_7^+$ ion formed from *trans*-2-butene with the reactant gases used in the $^{54}FeH^+$ studies were examined. In virtually all cases only collision-induced dissociation and proton transfer reactions were observed. The proton affinity of butadiene (assumed to be formed when $C_4H_7^+$ is de-

(5) (a) Dendramis, A.; Van Zee, R. J.; Weltner, W., Jr. *Astrophys. J.* **1979**, *231*, 632. (b) Van Zee, R. J.; Devore, T. C.; Wilkerson, J. L.; Weltner, W., Jr. *J. Chem. Phys.* **1978**, *69*, 1869. (c) Van Zee, R. J.; Devore, T. C.; Weltner, W., Jr. *Ibid.* **1979**, *71*, 2051.

(6) Papers which have reported calculations on FeH include: (a) Das, G. *J. Chem. Phys.* **1981**, *74*, 5766. (b) Scott, P. R.; Richards, W. G. *Ibid.* **1975**, *63*, 1690. (c) Walker, J. H.; Walker, T. E. H.; Kelly, H. P. *Ibid.* **1972**, *57*, 2094.

(7) (a) Stevens, A. E.; Beauchamp, J. L. *Chem. Phys. Lett.* **1981**, *78*, 291. (b) Stevens, A. E.; Beauchamp, J. L. *J. Am. Chem. Soc.* **1981**, *103*, 190.

(8) Stevens, A. E.; Feigerle, C. S.; Lineberger, W. C. *J. Chem. Phys.* **1983**, *78*, 5420.

(9) Armentrout, P. B.; Beauchamp, J. L. *Chem. Phys.* **1980**, *50*, 37.

(10) Armentrout, P. B.; Beauchamp, J. L. *J. Am. Chem. Soc.* **1981**, *103*, 784.

(11) Armentrout, P. B.; Halle, L. F.; Beauchamp, J. L. *J. Am. Chem. Soc.* **1981**, *103*, 6501.

(12) (a) Halle, L. F.; Armentrout, P. B.; Beauchamp, J. L. *Organometallics* **1982**, *1*, 963. (b) Byrd, G. D.; Burnier, R. C.; Freiser, B. S. *J. Am. Chem. Soc.* **1982**, *104*, 3565.

(13) Armentrout, P. B.; Beauchamp, J. L. *J. Chem. Phys.* **1981**, *74*, 2819.

(14) Moore, C. E. "Atomic Energy Levels"; National Bureau of Standards: Washington, D. C., 1949.

(15) Halle, L. F.; Armentrout, P. B.; Beauchamp, J. L. *J. Am. Chem. Soc.* **1981**, *103*, 962.

(16) Mysov, E. I.; Lyatifov, I. R.; Materikova, R. B.; Nochetkova, N. S. *J. Organomet. Chem.* **1979**, *169*, 301. We obtain a somewhat higher ratio of FeH^+:Fe^+ (~0.27) than is reported here.

protonated) is approximately the same as that derived for Fe in this study.[17] Cross sections for proton transfer were virtually identical for $C_4H_7^+$ and FeH^+ as reactants. Hence, the minor contamination of this species in the beam does not have a significant effect on our results.

The beam of ions of mass 57 amu from $(CH_3C_5H_4)_2Fe$ shows a very small amount of collision-induced fragmentation products at m/e 29 ($\sigma \sim 0.02$ Å^2) and m/e 31 ($\sigma \sim 0.006$ Å^2). These could be due to $C_4H_9^+$ formed in a complex rearrangement of the methylcyclopentadienyl rings upon electron impact or perhaps from ionization of the background gas.

The nominal collision energy of the ion beam is taken as the difference in potential between the collision chamber and either the center of the filament (determined by a resistive divider) of the surface ionization source or the gas chamber of the electron impact source. This collision energy is checked by use of a retarding field energy analyzer. Agreement was always within 0.3 eV for the surface ionized beam. The beam produced by the electron impact source has a less certain energy, which can vary up to 1.8 eV from the nominal value. This will not affect the trends observed for the exothermic reactions reported. In the one endothermic reaction studied, FeH^+ with D_2, the uncertainty caused by this energy is only 0.13 eV in the center of mass frame. By use of the retarding field analyzer, the energy distribution of the Fe^+ beam produced by surface ionization is 0.7 eV (fwhm), and that of the FeH^+ beam produced by electron impact of $(CH_3C_5H_4)_2Fe$ was less than 1.1 eV (fwhm). The effect of this spread in kinetic energy is small in the present experiments.

The effect of the thermal motion of the reactant gas in ion beam collision chamber experiments has been discussed in detail elsewhere.[18] The energy broadening due to this motion washes out any sharp features in reaction cross sections. For exothermic reactions this has little effect on the observed cross sections and branching ratios. Consequently, we report such data without taking this energy distribution into account. For endothermic reactions, the thermal motion obscures the threshold energy for reactions. By convoluting a functional form for the reaction cross section, $\sigma(E)$, with the thermal energy distribution, using the method of Chantry,[18] and fitting this new curve to the data, we take specific account of this factor.

Our choice for the functional form of the reaction cross section is discussed in detail elsewhere.[13] The form used, eq 1, has three variable

$$\sigma(E) = \sigma_0[(E - E_0)/E]^n \quad (1)$$

parameters: σ_0, an effective cross section; E_0, the energy threshold for reaction [taken equal to the difference in bond energies of the neutral reactant (bond broken) and ionic product (bond formed)]; and n. Equation 1 is expected to apply for energies below the threshold for dissociation of the product ion. This threshold corresponds to the energy of the bond broken in the neutral reactant. Detailed treatments of the effect of dissociation on the observed reaction cross section also have been discussed previously.[9,13,19]

Reaction cross sections for specific products, σ_i, are obtained using eq 2 and 3 which relate the total reaction cross section, σ, the number

$$I_0 = (I_0 + \Sigma I_i) \exp(-n_0 \sigma l) \quad (2)$$

$$\sigma_i = \sigma I_i / \Sigma I_i \quad (3)$$

density of the target gas, n_0, and the length of the collision chamber, l (5 mm), to the transmitted reactant ion beam intensity, I_0, and the sum of the product ion intensities, ΣI_i. The pressure of the target gas, measured using an MKS Baratron Model 90H1 capacitance manometer, is usually kept low, $<2.5 \times 10^{-3}$ torr, to minimize attenuation of the beam and ensure that reactions are the result of only a single bimolecular collision.

It is important to point out that neutral products are not detected in these experiments. However, except where noted below, the identity of these products can usually be inferred without ambiguity. In addition, these experiments provide no direct structural information about the ionic products. Thermochemical arguments can often distinguish possibilities for isomeric structures.

Results and Discussion

Reaction of Fe^+ with H_2, D_2, and HD. Iron ions react with H_2 to form FeH^+ as indicated in eq 4. The variation of the cross

$$Fe^+ + H_2 \rightarrow FeH^+ + H \quad (4)$$

section with energy for this reaction is shown in Figure 3 and is characteristic of an endothermic reaction. In analogy to previous studies of such metal-ion hydrogen systems, the data have been interpreted by using eq 1 with $n = 1$.[9,19] The fit shown in Figure 3 gives $\sigma_0 = 1.76$ Å^2 and $E_0 = 2.0 \pm 0.15$ eV, and is convoluted as discussed above. Combined with the bond energy of H_2, $D°(H_2) = 4.52$ eV, this threshold yields a value for $D°(Fe^+–H)$ of 2.52 ± 0.15 eV. At high energies the cross section for reaction 4 decreases owing to dissociation of FeH^+. This process has a thermodynamic threshold equal to the bond energy of H_2. The fit to the data above this energy uses an analysis discussed in detail elsewhere.[9,19]

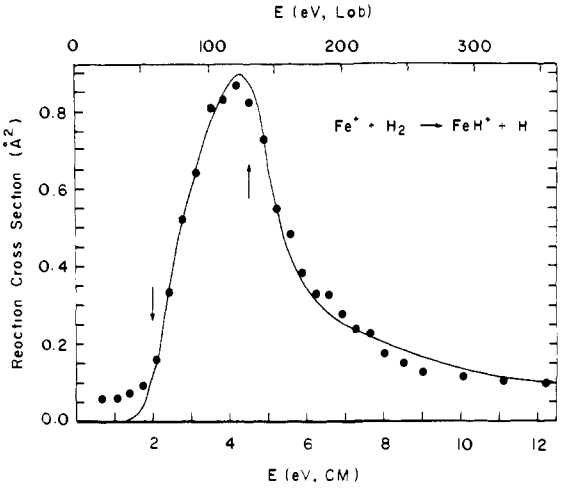

Figure 3. Variation in experimental cross section for reaction 4 as a function of kinetic energy in the center-of-mass frame (lower scale) and the laboratory frame (upper scale). The solid line is the fit to the data described in the text. Arrows mark the threshold energy at 2.0 eV, and the bond energy of H_2 at 4.52 eV.

The reaction of Fe^+ with D_2 was also studied, process 5. The

$$Fe^+ + D_2 \rightarrow FeD^+ + D \quad (5)$$

data for this reaction are not shown, but look very similar to those plotted in Figure 3. The cross section rises to a maximum of ~0.5 Å^2 at 4 eV relative kinetic energy. The best fit using eq 1 with $n = 1$ gives $\sigma_0 = 0.84$ Å^2 and $E_0 = 2.0 \pm 0.15$ eV. From this threshold and $D°(D_2) = 4.60$ eV, a value of $D°(Fe^+–D) = 2.60 \pm 0.2$ is determined. Making a zero-point energy correction of 0.03 eV[20] yields $D°(Fe^+–H) = 2.57 \pm 0.15$. Taking an average of the two determinations of the iron ion–hydrogen bond energy, a value of $D°(Fe^+–H) = 2.55 \pm 0.2$ eV (59 ± 5 kcal/mol) is obtained. This value agrees well with the limit, $D°(Fe^+–H) <$ 71 kcal/mol obtained by Allison and Ridge.[21] The proton affinity of the iron atom, PA(Fe), can be calculated from eq 6. The term

$$PA(Fe) = D°(Fe^+–H) + IP(H) - IP(Fe) \quad (6)$$

IP(X) denotes the ionization potential of species X. The proton affinity obtained, PA(Fe) = 190 ± 5 kcal/mol, is only slightly larger than those of the other first-row group 8 metals [PA(Co) = 184 ± 4 kcal/mol[10] and PA(Ni) = 180 ± 3 kcal/mol[9]].

The reaction of Fe^+ with HD was also briefly examined. The results are similar to the reaction of Ni^+ with HD in that formation of FeH^+ is favored over FeD^+ at all energies.[9] From threshold to the maximum of the FeH^+ peak, $\sigma \sim 0.34$ Å^2 at 4 eV relative kinetic energy, the cross section for FeH^+ ranges from three to four times that for FeD^+.

Reaction of FeH^+ with D_2. The reaction of FeH^+ with D_2 was examined in an attempt to further characterize a possible intermediate in reaction 4, namely FeH_2^+. In addition, we wished to probe the thermoneutral exchange reaction 7. No $FeHD^+$ was

$$FeH^+ + D_2 \rightarrow FeD^+ + HD \quad (7)$$

(17) Schultz, J. C.; Houle, F. A.; Beauchamp, J. L. *J. Am. Chem. Soc.*, submitted for publication.
(18) Chantry, P. J. *J. Chem. Phys.* **1971**, *55*, 2746.
(19) Armentrout, P. B.; Beauchamp, J. L. *Chem. Phys.* **1980**, *48*, 315.
(20) A vibrational frequency of FeH^+ of 1629 cm^{-1} was used: Schilling, J. B.; Goddard, W. A., III, unpublished results.
(21) Allison, J.; Ridge, D. P. *J. Am. Chem. Soc.* **1979**, *101*, 4998.

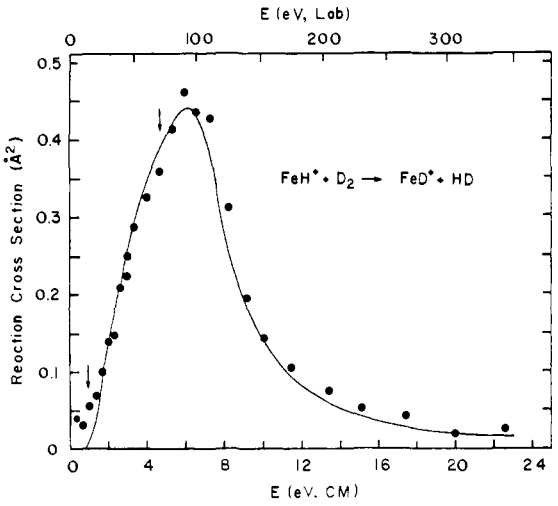

Figure 4. Variation in experimental cross section for reaction 7 as a function of kinetic energy in the center-of-mass frame (lower scale) and the laboratory frame (upper scale). The solid line is the fit to the data described in the text. Arrows mark the threshold energy at 0.9 eV and the bond energy of D_2 at 4.6 eV.

observed in the reaction of FeH^+ with D_2. If D_2 does add to FeH^+ to form **1**, an Fe(IV) species, then the energetics for reductive

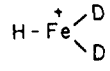

1

elimination of molecular hydrogen (HD or D_2) are probably more favorable than for cleavage of an Fe^+–H or Fe^+–D bond. It is interesting to note that while dihydrides of nickel ions are present in slow field tip evaporation studies, no FeH^+ or FeH_2^+ is observed.[22] If the latter ion is formed, rapid reductive elimination of H_2 may prevent its observation.

Data for the exchange reaction 7 are presented in Figure 4. The maximum cross section is quite low for a thermoneutral reaction, $\sigma_{max} < 0.54$ Å^2. In addition, the variation of the cross section with energy indicates a substantial activation energy for this reaction. The fit to the data shown in Figure 4 uses eq 1 with $n = 3$, $\sigma_0 = 0.73$ Å^2, and $E_0 = 0.9$ eV. This threshold, $E_0 = 20 \pm 7$ kcal/mol, is equal to the activation energy for this process.

Two possibilities exist for the intermediate of reaction 7. The first is formed by oxidative addition of D_2 to the metal center to form the Fe(IV) species, **1**. This is not a preferred oxidation state of the metal. Another possible structure is a four-centered intermediate, **2**. The exchange reactions with D_2 of Cl_2M–H, M

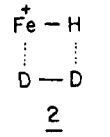

2

= Sc, Ti, Ti^+, proceeding through a structure analogous to **2** have been studied by Steigerwald and Goddard using generalized valence-bond methods.[23] These calculations indicate that the activation barrier for this process will be large for systems with a large amount of metal s or p character in the M–H bond. Correlation of experimental metal ion–hydrogen bond strengths with electronic promotion energies of the metal ion indicate that the metal orbital in the Fe^+–H bond is primarily s in character.[11] This is supported by preliminary calculations on the FeH^+ molecule.[24] Given these considerations, both structures **1** and **2** are expected to be high-energy intermediates, consistent with the experimental observation of a large activation barrier for reaction 7. The experiments do not distinguish the two possibilities.

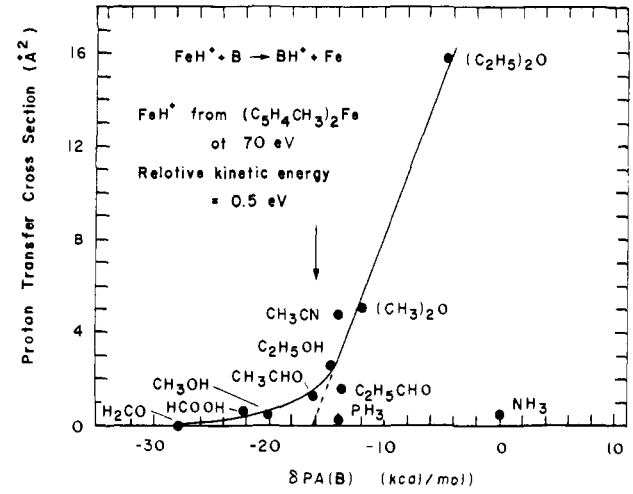

Figure 5. Experimental cross sections for reaction 8 plotted as a function of the proton affinity of base. All measurements shown were taken at ~0.5 eV relative kinetic energy. The arrow marks δPA(Fe) calculated from the thresholds of reactions 4 and 5, and assuming $PA(NH_3) = 204$ kcal/mol.

Proton Transfer Reactions of FeH^+. In the studies reported above, the proton affinity of Fe was determined by measuring the energy required to form FeH^+ from the reaction of Fe^+ with hydrogen. A complementary method of determining this value is to measure the energy required to remove a proton from FeH^+. This can be accomplished by using the ion beam apparatus to measure the cross section for proton transfer from FeH^+ to bases of varying proton affinity (process 8). The enthalpy change for this process is given in eq 9.

$$FeH^+ + B \rightarrow Fe + BH^+ \quad (8)$$

$$\Delta H = PA(Fe) - PA(B) \quad (9)$$

Proton transfer processes are commonly observed in gas-phase studies of the reactions of organic ions with n-donor bases.[25] The observation of large cross sections for reaction 8 would be consistent with an exothermic process. Endothermic proton transfer reactions can be made to occur by supplying excess translational energy to the system. The variation of cross section for reaction 8 with relative kinetic energy was examined for bases of varying proton affinities.[25] Formaldehyde has the lowest proton affinity of the bases used, δPA = −27.8 kcal/mol, where the proton affinity is given relative to ammonia, eq 10. The best estimate for

$$\delta PA(B) = PA(B) - PA(NH_3) \quad (10)$$

$PA(NH_3)$ is discussed below. No ion corresponding to CH_2OH^+ was observed at low energies in the reaction of FeH^+ with formaldehyde, and only a very small amount (~0.04 Å^2) of this product appeared at a higher energy (~2 eV relative kinetic energy). The proton transfer cross section for reaction of FeH^+ with methanol, δPA = −20.1 kcal/mol, is ~0.3 Å^2 at the lowest energy measured (~0.09 eV in the center-of-mass frame (CM)), increases slowly to a maximum of ~0.7 Å^2 at ~1.8 eV (CM), and then decreases. This suggests the reaction is slightly endothermic. The behavior of the cross section for reaction 8 with bases having $\delta PA \geq \delta PA(CH_3CHO) = 16.1$ kcal/mol is characteristic of exothermic processes, suggesting a value for δPA(Fe) between −20.1 and −16.1 kcal/mol.

A comparison of the proton transfer cross sections for the various bases measured at the same interaction energy, ~0.5 eV (CM), is shown in Figure 5. The cross section for reaction 8 is

(22) Kapur, S.; Müller, E. W. *Surf. Sci.* **1977**, *66*, 45.
(23) Steigerwald, M. L.; Goddard, W. A., III, to be submitted for publication.
(24) Preliminary calculations indicate that the hybridization of the metal orbital involved in the Fe^+–H bond is 75% s, 11% p, and only 14% d: Schilling, J. B.; Goddard, W. A., III, unpublished results.
(25) Aue, D. H.; Bowers, M. T. In "Gas Phase Ion Chemistry"; Bowers, M. T., Ed.; Academic Press: New York, 1979; Vol. 2. Values for δPA were taken from this reference.

plotted for each base according to its proton affinity relative to ammonia. Overall, the trend is as expected, with higher cross sections for the bases with higher proton affinities. The line shown is a least-squares fit to the data in the range of $\delta PA = -16.1$ kcal/mol to $\delta PA = -4$ kcal/mol. These data appear to extrapolate to a value of $\delta PA = -16.0$ kcal/mol, which can be considered as an estimate of the threshold for the proton transfer reaction to occur. However, there are numerous competing reactions discussed below which complicate any quantitative analysis. It is not clear why the proton transfer cross section for the group 5 bases are low. While the reaction with PH_3 may be only thermoneutral, proton transfer to ammonia should be highly exothermic. Formation of $Fe(NH_2)^+$ and the adduct $HFe(NH_3)^+$ does occur in the reaction with ammonia. It is possible that coordination to the metal cation ties up the site to which the proton can be transferred, in which case the presence of an additional lone pair in the base may be required to observe proton transfer near the thermodynamic threshold.[26] If such an adduct is formed, the reductive elimination of NH_4^+ may have a sizable activation barrier relative to loss of NH_3 to regenerate the reactants.

An absolute value for the proton affinity of Fe is determined from the proton affinity of ammonia. Photoionization appearance potential measurements of NH_4^+ from NH_3 dimers made by Ceyer et al. yield a value of $PA(NH_3) = 203.6$ kcal/mol[27] (298 K) though other estimates are higher.[28] Combining $PA(NH_3) = 204 \pm 2$ kcal/mol with $\delta PA(Fe) = 16$ kcal/mol yields a value for the proton affinity of Fe, $PA(Fe) = 188$ kcal/mol. This number agrees very well with the above determination, $PA(Fe) = 190 \pm 5$, derived from the Fe^+–H bond energy.

As noted in the Experimental Section, FeH^+ formed by electron impact of the 1,1′-dimethylferrocene may possess excess vibrational energy. The agreement between the values for the proton affinity of Fe derived from threshold measurements of the reactions of Fe^+ with H_2 and D_2 and from proton transfer reactions of FeH^+ suggests that the latter ion has little vibrational excitation. If it were vibrationally excited, the proton transfer studies would lead to a lower proton affinity for Fe.

Hydride Transfer Reactions of FeH^+. In addition to proton transfer from FeH^+ to the above bases, the interaction with these compounds can also result in a hydride ion being transferred from the neutral reactant to FeH^+, to form FeH_2 (reaction 11).

$$FeH^+ + AH \rightarrow FeH_2 + A^+ \qquad (11)$$

Reaction 11 will occur when the hydride affinity of FeH^+, $D[HFe^+–H^-]$, is greater than that of A^+ (where AH in eq 11 represents the base). The enthalpy for reaction 11 is given in eq 12.

$$\Delta H = D[A^+–H^-] - D[HFe^+–H^-] \qquad (12)$$

Table I lists $D[A^+–H^-]$ for all species AH used in the present studies. Appreciable yields of A^+, reaction 11, are observed for the first four compounds listed. The cross section for formation of A^+ at low energies in the reaction of FeH^+ with AH = CH_3CH_2OH is less than 0.4 Å^2 and varies only slightly with kinetic energy. Hydride transfer from $(CH_3)_2O$ to FeH^+ exhibits characteristics of an endothermic reaction, with the cross section increasing with increasing kinetic energy (the threshold could not be accurately determined). These results suggest that a lower limit of 232 kcal/mol can be taken for $D[HFe^+–H^-]$. Hydride transfer reactions are often fast (at 300 K) and reversible and do not require activation energies in excess of their endothermicities.[32] This suggests that the lower limit is a measure of the true value. This result gives $\Delta H_f(FeH_2) < 77.5$ kcal/mol, from which an enthalpy change greater than 22 kcal/mol is calculated for process 13. Thus, the sum of the first two hydrogen bonds to an iron

$$FeH_2 \rightarrow Fe + H_2 \qquad (13)$$

atom is greater than 126 kcal/mol. Earlier experimental and theoretical estimates for the Fe–H bond dissociation energy range from 23 to 55 kcal/mol.[5a,6,33] Freiser and co-workers[34] have recently shown that collision-induced dissociation of transition metal carbonyl anions leads to formation of bare metal anions. Determination of the acidity of the corresponding metal hydride by examining proton abstraction reactions of the metal anion leads to homolytic bond dissociation. Preliminary results for iron give $D[Fe–H] = 30 \pm 3$ kcal/mol.[35] This low value implies $D[H–Fe–H] > 96$ kcal/mol, which seems remarkably high. From electron photodetachment studies of FeD^-, Stevens et al. propose that FeH has a $^4\Delta$ ground state.[8]

Sweany has observed oxidative addition of H_2 to $Fe(CO)_4$ in matrix isolation studies, which suggests there is little or no activation energy for this process.[36] The activation energy for the reverse reaction, reductive elimination of H_2 from $H_2Fe(CO)_4$, has been calculated from kinetic studies by Pearson and Mauermann to be 26 kcal/mol.[37] The above two studies indicate that the enthalpy change for addition of H_2 to $Fe(CO)_4$ is ~26 kcal/mol. It is interesting to note that even though the molecular

Table I. Calculated Bond Strengths for Hydride Transfer Reagents

AH[a]	$D(A^+–H^-)$[b-d] (kcal/mol)	AH[a]	$D(A^+–H^-)$[b-d] (kcal/mol)
$(CH_3CH_2)_2O$	214[e]	CH_3OH	255
CH_3NH_2	218	HCOOH	267
CH_3CH_2CHO	224	PH_3[i]	295
CH_3CHO	231.4[f]	CH_3CN	306
CH_3CH_2OH	231.9[g]	NH_3[i]	348
$(CH_3)_2O$	236[h]		

[a] Heats of formation for organic compounds taken from ref 31 unless noted. [b] The lowest value for $D(A^+–H^-)$ is listed for compounds with different types of hydrogen bonds. [c] These values are calculated using a value for the electron affinity of H, EA(H) = 0.754 eV, from: Wagman, D. D.; Evans, W. H.; Parker, V. B.; Harlow, I.; Bailey, S. M.; Schumm, R. H. *Natl. Bur. Stand. Tech. Note* 1968, No. 270-3. [d] Heats of formation or selected appearance potentials for ions are taken from: Rosenstock, H. M.; Draxl, K.; Steiner, B. W.; Herron, J. T. *J. Phys. Chem. Ref. Data, Suppl.* 1977, *6*, No. 1, unless otherwise noted. [e] Calculated using appearance potential measurement of $C_4H_9O^+$ from i-$C_3H_7OC_2H_5$ from reference listed in footnote *h* of this table. ΔH_f(i-$C_3H_7OC_2H_5$) taken to be the average of $\Delta H_f[(C_2H_5)_2O]$ and $\Delta H_f(i\text{-}C_3H_7)_2O$ from ref 31. [f] $\Delta H_f(CH_3CO^+) = 157.0 \pm 0.4$ kcal/mol from: Traeger, J. C.; McLoughlin, R. G.; Nicholson, A. J. C. *J. Am. Chem. Soc.* 1982, *104*, 5318. [g] $\Delta H_f(C_2H_5OH^+) = 141$ kcal/mol from: Rafaey, K. M. A.; Chupka, W. A. *J. Chem. Phys.* 1968, *48*, 5205. [h] $\Delta H_f(CH_3OCH_2^+) = 157$ kcal/mol from: Lossing, F. P. *J. Am. Chem. Soc.* 1977, *99*, 7526. [i] Heat of formation taken from reference listed in footnote *d* of this table.

(26) Failure to observe formation of ammonia in the reaction of protonated methylamine with methylamine may be due to this same phenomenon if the reaction proceeds through a four-centered front-sided displacement mechanism: Beauchamp, J. L. In "Interactions between Ions and Molecules"; Ausloos, P., Ed.; Plenum: New York, 1975; Vol. 6.

(27) Ceyer, S. T.; Tiedemann, P. W.; Mahan, B. H.; Lee, Y. T. *J. Chem. Phys.* **1979**, *70*, 14.

(28) Lias et al. have determined $\delta PA(i\text{-}C_4H_8) = 8.2$ kcal/mol (Lias, S. G.; Shold, D. M.; Ausloss, P. *J. Am. Chem. Soc.* **1980**, *102*, 2540). Using the value of $IP(t\text{-}C_4H_9\cdot) = 6.70$ eV[29] and $\Delta H_f(t\text{-}C_4H_9\cdot) = 8.7$ kcal/mol[30] gives $PA(NH_3) = 206.7$ kcal/mol. If a higher heat of formation of the radical is used, $\Delta H_f(t\text{-}C_4H_9\cdot) = 12.2$ kcal/mol (Tsang, W. *Int. J. Chem. Kinet.* **1978**, *10*, 821), then the value $PA(NH_3) = 203.1$ kcal/mol is obtained. This lower value gives better agreement between values of $\delta PA(H_2O)$ derived from a recent determination of $PA(H_2O)$, and earlier studies (Collyer, S. M.; McMahon, T. B. *J. Phys. Chem.*, submitted for publication).

(29) Houle, F. A.; Beauchamp, J. L. *J. Am. Chem. Soc.* **1979**, *101*, 4067.

(30) McMillen, D. F.; Golden, D. M. *Annu. Rev. Phys. Chem.* **1982**, *33*, 493.

(31) Heats of formation for hydrocarbons taken from: Cox, J. D.; Pilcher, G. "Thermochemistry of Organic and Organometallic Compounds"; Academic Press: New York, 1970.

(32) Meot-Ner, M.; Field, F. H. *J. Chem. Phys.* **1976**, *64*, 277.

(33) Carroll, P. K.; McCormack, P.; O'Connor, S. *Astrophys. J.* **1976**, *208*, 903.

(34) Sallans, L.; Lane, K.; Squires, R. R.; Freiser, B. S. *J. Am. Chem. Soc.* **1983**, *105*, 6352.

(35) Freiser, B. F., private communication.

(36) Sweany, R. L. *J. Am. Chem. Soc.* **1981**, *103*, 277.

(37) Pearson, R. G.; Mauermann, H. *J. Am. Chem. Soc.* **1982**, *104*, 500.

and electronic structure of this system is very different from the FeH_2 species, the overall energetics of reductive elimination are comparable. Ozin and co-workers point out that oxidative addition of H_2 to Fe atoms in a cryogenic matrix is observed only as a photoactivated process.[38] This result suggests that reaction 13 has an activation barrier in excess of the estimated 22 kcal/mol endothermicity. Infrared studies of FeH_2, FeD_2, and FeHD suggest a bent structure for the dihydride.[38]

Reactions of FeH^+ with Alkanes. The reactions of FeH^+ with methane, ethane, and butane were studied at low energies. The purpose of these experiments was to examine the occurrence of reaction 14. Labeled substrates would then allow the site of

$$FeH^+ + RH \rightarrow FeR^+ + H_2 \quad (14)$$

reaction to be identified. Methane-d_4 was used to check for the deuterium exchange reaction leading to FeD^+. No products were observed at low energies with methane or ethane, despite the fact that reaction 15 is nearly thermoneutral and reactions 16 and 17

$$FeH^+ + CD_4 \rightarrow FeD^+ + CHD_3 \quad (15)$$

$$\rightarrow FeCD_3^+ + HD \quad (16)$$

$$FeH^+ + C_2H_6 \rightarrow FeCH_3^+ + CH_4 \quad (17)$$

are exothermic by 10 and 24 kcal/mol, respectively.[39] Failure to observe these reactions is perhaps not surprising since the thermoneutral exchange reaction with D_2 occurs with a significant activation energy. Accordingly, reaction 17 was observed at higher energies (the threshold was not examined). In analogy to the D_2 exchange reaction discussed earlier, the high-energy intermediate involved in these reactions may either be an Fe(IV) species or a four-centered intermediate.

At low energies FeH^+ reacts with butane to yield $Fe(C_4H_9)^+$ and $Fe(C_4H_7)^+$, processes 18 and 19. The total reaction cross

$$FeH^+ + n\text{-}C_4H_{10} \xrightarrow{73\%} Fe(C_4H_9)^+ + H_2 \quad (18)$$

$$\xrightarrow{27\%} Fe(C_4H_7)^+ + 2H_2 \quad (19)$$

section at 0.5 eV is less than 3 Å^2. No products formed via carbon–carbon bond cleavage are observed. While D-$[(CH_3)(C_2H_5)CH^+\text{–}H^-]$ is equal to 246 kcal/mol,[30,31,40] the enthalpy change for process 20 is only 229 kcal/mol,[29-31] which is

$$n\text{-}C_4H_{10} \rightarrow t\text{-}C_4H_9^+ + H^- \quad (20)$$

less than the lower bound determined above for $D[HFe^+\text{–}H^-]$. Thus, it is not unreasonable that the first step in the dehydrogenation reaction is hydride transfer to FeH^+ accompanied by rearrangement of the resulting carbocation. This mechanism would not occur for methane or ethane since $D[H_3C^+\text{–}H^-] = 315$ kcal/mol and $D[(CH_3)_2CH^+\text{–}H^-] = 248$ kcal/mol.[29] Processes analogous to reactions 18 and 19 are observed with isobutane as the hydrocarbon reactant, with a product distribution of 97 and 3%, respectively.

In contrast to the above reactions of FeH^+, bare iron ions oxidatively add to carbon–carbon and carbon–hydrogen bonds of alkanes larger than ethane in facile exothermic processes.[12] The resulting metal–dialkyl or metal–hydridoalkyl can undergo a β-hydrogen transfer to the metal leading to reductive elimination of H_2 or an alkane. At the same energy at which the FeH^+ reaction with butane was performed, the cross section for dehydrogenation of butane by Fe^+ is ~10 Å^2, while that for the loss of alkanes is ~30 Å^2.[12]

Reaction of FeH^+ with C_2D_4. The insertion of olefins into metal–hydrogen bonds is a reaction of great interest to organometallic chemists. In order to determine whether this reaction

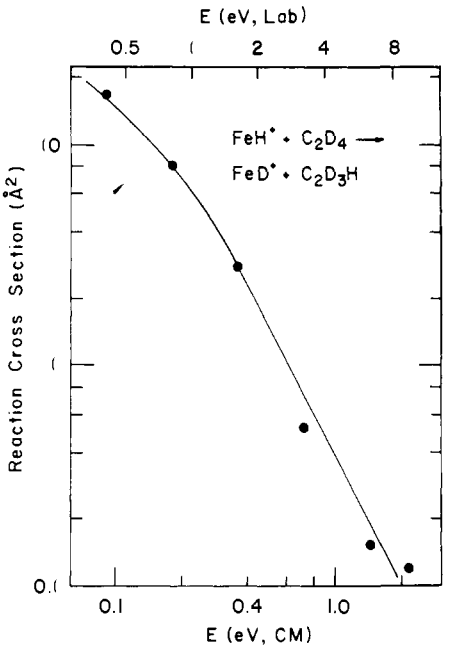

Figure 6. Variation in experimental cross section for reaction 21 as a function of kinetic energy in the center-of-mass frame (lower scale) and laboratory frame (upper scale).

Scheme I

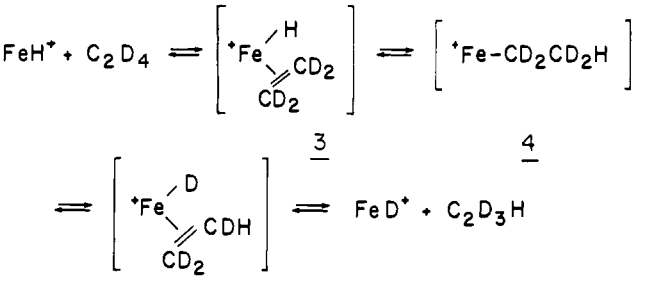

would occur in our gas-phase system, the reaction of FeH^+ with C_2D_4 was examined. The only product observed was due to the exchange reaction 21. The cross section for this reaction, shown

$$FeH^+ + C_2H_4 \rightarrow FeD^+ + C_2HD_3 \quad (21)$$

in Figure 6, is moderately high at low energies and decreases rapidly with increasing energy. The reaction exhibits no barrier, indicating that high-energy intermediates are not involved. The likely mechanism by which this reaction occurs is presented in Scheme I. The ethene molecule initially interacts with FeH^+ to form the π-bound complex, **3**, after which the familiar olefin insertion can occur to form the metal alkyl species **4**. The reaction continues by a β-deuterium transfer followed by elimination of ethene-d_3. This mechanism does not require Fe(IV) intermediates.

Complex Reactions of FeH^+ with Oxygen Bases. In the course of examining the proton and hydride transfer processes discussed above, additional products resulting from interaction of FeH^+ with alcohols, aldehydes, and ethers were observed at low energies. These reactions are listed in Table II. In addition, adduct formation is observed in all of these reactions, as might be expected from previous studies of cationic metal systems with oxygenated compounds.[41]

The reactions listed in Table II are generally complex, involving considerable rearrangement of bonds in the reaction intermediates. In the absence of labeling data, the mechanisms by which these reactions occur cannot be determined. Possibilities include oxidative addition processes or reactions typical of a Lewis acid. Though oxidative addition processes would involve formation of

(38) Ozin, G. A.; McCaffrey, J. G.; McIntosh, D. F.; Parnis, J. M.; Huber, H. X.; Gracie, C. *Angew. Chem.*, submitted for publication.
(39) $D°[Fe^+\text{–}CH_3] = 69 \pm 5$ kcal/mol from ref 12a.
(40) IP[*sec*-C_4H_9•] = 7.25 ± 0.03 eV: Schultz, J. C.; Houle, F. A.; Beauchamp, J. L., to be submitted for publication.
(41) Halle, L. F.; Crowe, W. E.; Armentrout, P. B.; Beauchamp, J. L., to be submitted for publication.

Table II. Exothermic Reactions of FeH^+ with Alcohols, Aldehydes, and Ethers[a]

	% of total reaction[b]	σ_{total} ($Å^2$)
Alcohols		
$FeH^+ + CH_3OH$		
$\rightarrow Fe + CH_3OH_2^+$	19	3
$\rightarrow FeOCH_3^+ + H_2$	81	
$FeH^+ + CH_3CH_2OH$		
$\rightarrow Fe + CH_3CH_2OH_2^+$	7	40
$\rightarrow FeOH^+ + C_2H_6$[c]	42	
$\rightarrow HFe(OH_2)^+ + C_2H_4$	51	
Aldehydes		
$FeH^+ + CH_3CHO$		
$\rightarrow Fe + CH_3CHOH^+$	30	10
$\rightarrow FeH_2 + CH_3CO^+$	5	
$\rightarrow FeCH_3^+ + (H_2 + CO)$[d,e]	44	
$\rightarrow Fe(COCH_3)^+ + H_2$	21	
$FeH^+ + CH_3CH_2CHO$		
$\rightarrow Fe + CH_3CH_2CHOH^+$	6	130
$\rightarrow Fe(C_2H_5)^+ + (H_2 + CO)$[d]	11	
$\rightarrow Fe(CHO)^+ + C_2H_6$		
$\rightarrow HFe(CH_2O)^+ + C_2H_4$	12	
$\rightarrow HFe(C_2H_6)^+ + CO$		
$\rightarrow Fe(COC_2H_5)^+ + H_2$	71	
Ethers		
$FeH^+ + (CH_3)_2O$		
$\rightarrow Fe + (CH_3)_2OH^+$	31	20
$\rightarrow FeH_2 + CH_3OCH_2^+$	<1	
$\rightarrow FeOCH_3^+ + CH_4$	69	
$FeH^+ + (CH_3CH_2)_2O$		
$\rightarrow Fe + (CH_3CH_2)_2OH^+$	16	200
$\rightarrow FeH_2 + CH_3CH_2OCHCH_3^+$	39	
$\rightarrow FeOC_2H^+ + C_2H_6$	28	
$\rightarrow HFe(C_2H_5OH)^+ + C_2H_4$	17	

[a] Measured at ~0.2–0.3 eV relative kinetic energy. [b] Adduct formation is not included in calculating these product distributions. [c] Using $D°(Fe^+–OH) = 76 \pm 5$ kcal/mol (from: Murad, E. *J. Chem. Phys.* 1980, *73*, 1381), an enthalpy change of $\Delta H_{rxn} = 24$ kcal/mol is calculated for this reaction (see ref 30 and 31). [d] The neutral products of this reaction may be either H_2CO or H_2 and CO. [e] Assuming the neutral products are H_2 and CO, the enthalpy change for this reaction is calculated to be $\Delta H_{rxn} = -13$ kcal/mol (see ref 30, 31, and 36).

Fe(IV) intermediates, these species may not be as unfavorable with the oxygenated compounds as with the hydrocarbon systems described above.[42,43] As a Lewis acid, FeH^+ may first abstract a hydride ion[21] or it may bind to n-donor bases followed by four-center rearrangements such as shown in Scheme II for an alcohol or ether. Scheme IIb is analogous to mechanisms proposed for the decomposition of proton-bound dimers of alcohols[44] and ethers.[45] In these reactions of FeH^+, the initially formed adduct may consist of a proton-bound alcohol or ether to an iron atom. The role of strong hydrogen bond formation in providing chemical activation of intermediates and lending stability to products has been previously noted in gas-phase studies of the reactions of organic ions.[46]

Scheme II

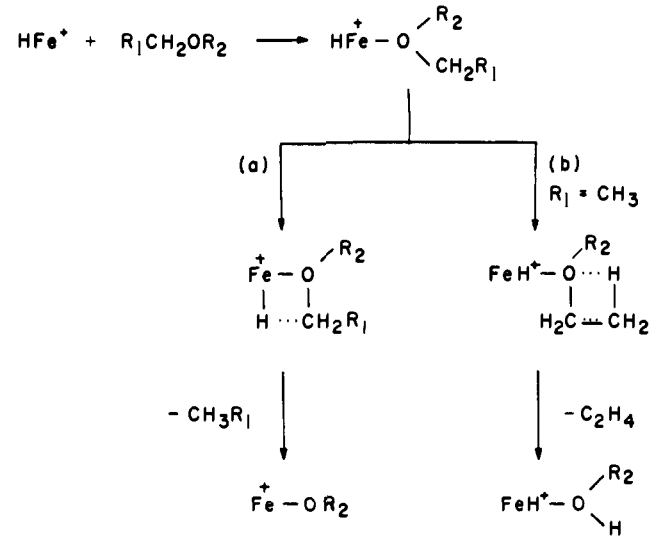

Conclusion

The present studies represent the first effort to extend our ion beam investigations of reactive intermediates in organometallic chemistry from atomic metal ions to organometallic fragments, the simplest of which is a metal hydride. The main results include (1) determination of the bond dissociation energy $D[Fe^+–H]$ by analyzing endothermic thresholds for reaction of Fe^+ with H_2 and D_2, (2) confirmation of this result by deprotonation of FeH^+ with a range of n-donor bases of varying strength, (3) demonstration that FeH_2 is stable with respect to the reductive elimination of H_2 by examining hydride abstraction reactions of FeH^+, (4) demonstration that oxidative addition of FeH^+ to H_2 or hydrocarbons to give Fe(IV) intermediates (or reaction via four-centered intermediates) is not a favorable process, and (5) observation that reversible insertion of olefins into the FeH^+ bond is a facile process. Reactions of FeH^+ with oxygenated species suggest some complex and interesting reactions which warrant further study. Electron impact of 1,1′-dimethylferrocene provides a less than ideal source of FeH^+. While this work was in progress, Freiser and coworkers[47] discovered that collision-induced dissociation of the initially formed product $FeOCD_3^+$ of the reaction of Fe^+ with CD_3ONO generates FeD^+ in good yield. They have reported preliminary ion cyclotron resonance studies of the reactions of this species with small molecules which are in good agreement with our ion beam experiments.

We are currently developing several new sources for the ion beam apparatus which should permit routine preparation of a wide range of organometallic fragments, including metal hydrides and alkyls. The present results indicate that ion beam studies of these species will reveal a rich and interesting chemistry and serve to characterize better the thermochemistry of reactive intermediates in catalytic processes.

Acknowledgment. The authors would like to thank Professor D. P. Ridge for suggesting the use of 1,1′-dimethylferrocene to generate the FeH^+ beam. This research was supported in part by the U.S. Department of Energy. Graduate fellowship support from Bell Laboratories, SOHIO, and the Shell Companies Foundation (L.F.H.) is gratefully acknowledged.

(42) For example, model porphyrin complexes have been prepared which contain an Fe(IV) unit: La Mar, G. N.; de Ropp, J. S.; Lechoslaw, L.-G.; Balch, A. L.; Johnson, R. B.; Smith, K. M.; Parish, D. W.; Cheng, R. J. *J. Am. Chem. Soc.* **1983**, *105*, 782.
(43) Atomic iron ions are observed to add to C–OH bonds of alcohols (ref 21).
(44) Bomse, D. S.; Beauchamp, J. L. *J. Am. Chem. Soc.* **1981**, *103*, 3292.
(45) Bomse, D. S.; Woodin, R. L.; Beauchamp, J. L. *J. Am. Chem. Soc.* **1979**, *101*, 5503.
(46) Ridge, D. P.; Beauchamp, J. L. *J. Am. Chem. Soc.* **1971**, *93*, 5925.
(47) Carlin, T. J.; Sallans, L.; Cassady, C. J.; Jacobson, D. B.; Freiser, B. S. *J. Am. Chem. Soc.* **1983**, *105*, 6321.